Stabilization of quasiperiodic orbits for line-coupled diode resonator systems

Z. Yu, J. Steinshnider, C. L. Littler, J. M. Perez, and J. M. Kowalski
Physics Department, University of North Texas, Denton, Texas 76203
(Received 25 June 1993)

Chaotic transitions in line-coupled diode resonator systems were experimentally found to follow the Curry-Yorke model [*The Structure of Attractors in Dynamical Systems* (Springer, Berlin, 1977), p. 48]. The standard diode model from the computer program SPICE was used to simulate these systems; the complete Lyapunov spectra from simulated systems are in good agreement with the spectra computed from the experimental time series. By applying the proportional-feedback technique to these systems, we can stabilize periodic orbits of increasing periods as well as unstable quasiperiodic orbits densely covering a torus.

PACS number(s): 05.45.+b

Soon after Ott, Grebogi, and Yorke [1] proposed a stabilization scheme for unstable periodic orbits embedded in a chaotic attractor, several experiments on different dynamical systems were reported [2] where these ideas were used to convert a chaotic attractor into a specific generator of periodic signals with period $T, 2T, \ldots, nT, \ldots$. In particular, a single-diode resonator circuit driven by an external harmonic signal has been studied by Hunt [3]. The source of nonlinearity in the system is a *pn*-junction diode. It is known that this system becomes chaotic via a period-doubling route [4]. Using a modified stabilization scheme (called a "proportional-feedback technique") Hunt was able to stabilize periodic orbits up to period 23. It is also known that higher-dimensional line-coupled diode resonator systems of this type can reach the chaotic state via a different route through quasiperiodic regimes [5]. The best known route of this type is the classical Ruelle-Takens scenario: periodic solution $\rightarrow$ stable T^2 (quasiperiodic behavior with two incommensurate frequencies) $\rightarrow$ stable T^3 (three incommensurate frequencies) $\rightarrow$ chaos. However, as pointed out by Curry and Yorke [6], direct transition from T^2 to chaos is also possible.

Our experiments with line-coupled circuits and subsequent analyses of time series indicate that the Curry-Yorke model describes the chaotic transition in these systems. To model the line-coupled system, we have used the standard model of a diode as a nonlinear capacitance in parallel with a nonlinear conductor as described in the computer simulation program SPICE [7] (see the Appendix). Calculations of Lyapunov spectra from experimental time series and spectra from the SPICE simulated system are compared and found in good agreement. More importantly, we show that the proportional-feedback technique can be applied to stabilize unstable quasiperiodic orbits in the experimental line-coupled systems in addition to periodic orbits in the single-resonator systems.

The line-coupled system of two diode resonators is presented in Fig. 1. The frequency of the driving signal was typically set near the 50-KHz range. The voltage V_1 across resistance R_1 was measured via a differential amplifier with high input impedance. This voltage is considered as a generic variable allowing one to reconstruct the system's dynamics by the well-known method of embedding in the space of delayed signals [8]. We restricted ourselves to continuous monitoring of two-dimensional projections of orbits in the embedding space, i.e., we fed the output voltage $V_1(t)$ and its copy $V_1(t+\tau)$ to two channels of an oscilloscope in the X-Y mode. Additionally, a pulse generator was used to create pulses at the peak positions of the driving signal. This pulse generator consisted of a differentiator and a zero-crossing detector. We used these pulses to strobe the Z axis of the oscilloscope and thus display the Poincaré sections of phase plots. Time series data were taken by an Analog Devices Model FAST-16 series digitizer with 16-bit resolution, 1 MHz speed, and 1 M-word memory.

For an increasing amplitude of the driving signal with fixed frequency $f_0 = 53.21$ KHz the following sequence has been observed. (1) For the driving amplitude $V_0 \leq 6.07$ V the system resides on a simple stable limit cycle with frequency equal to the driving frequency (period-1 "oscillations" of the system). (2) For 6.07 V $\leq V_0 \leq 9.87$ V the system has a quasiperiodic attractor (two-dimensional torus). (3) For 9.87 V $\leq V_0 \leq 10.50$ V the system appears to be chaotic. (4) The chaotic regime is followed by clear period-3 stable oscillations that occur

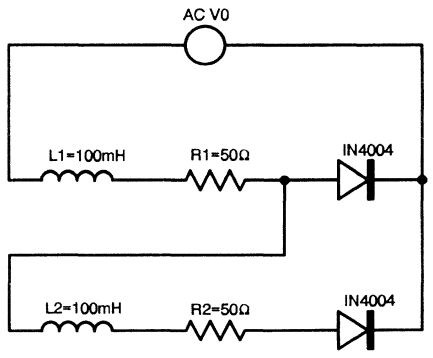

FIG. 1. Schematic diagram of the line-coupled diode resonator system. R_1 and R_2 are 50-Ω resistors, L_1 and L_2 are 100-mH inductors. The sinusoidal driving voltage was supplied by a Tektronix Model SG 505 oscillator.

for 10.50 V $\leq V_0 \leq 13.00$ V. The Poincaré section of the system, experimentally obtained as described above, is represented by three bright dots in Fig. 2(a). (5) Further increase in the amplitude of the driving signal, when 13.01 V $\leq V_0 \leq 14.21$ V, brings the system again to a different two-frequency quasiperiodic attractor, with period-3 windows as shown in Fig. 2(b). Poincaré sections of these tori consist of three nearly circular closed curves, centered on the three dots of the periodic orbit as in Fig. 2(a). The radii of the circles grow rapidly with increasing amplitude of the driving signal. The power spectrum of this regime is shown in Fig. 3(a), where one can identify the fundamental frequency f_0 and another incommensurate frequency f_1 with all other frequencies occurring at linear combinations of f_0 and f_1 with rational multipliers. The value of f_1 slowly increases with an increase of the amplitude V_0. (6) For yet higher driving amplitudes, 14.25 V $\leq V_0 \leq 15.31$ V, we observed frequency-locked states, Fig. 2(c), with an orbit of high period residing on the torus. The Poincaré section initially consists of three groups of dots falling on nearly circular closed curves. These closed curves deformed away from circles with increasing V_0. The power spectrum shown in Fig. 3(b) shows that all peaks occur at frequencies $(p/q)f_0$ where p and q are integers and a particularly strong peak is observed at the period-3 positions. The frequency-locking ratio is $f_0/f_1 = \frac{33}{3}$. (7) Finally, with further increase of the driving voltage (15.40 V $\leq V_0 \leq 16.20$ V) we again reached the chaotic regime, shown in Fig. 2(d). The attractor still bears a resemblance to that in the quasiperiodic regime, but the presence of wrinkles and corrugations indicates that folding is taking place. Broadband features, seen in the power spectrum with period-3 windows, are shown in Fig. 3(c). This sequence of transitions agrees with the Curry-Yorke scenario [6].

Additional evidence for the existence of chaotic and quasiperiodic regimes can be provided, as usual, by

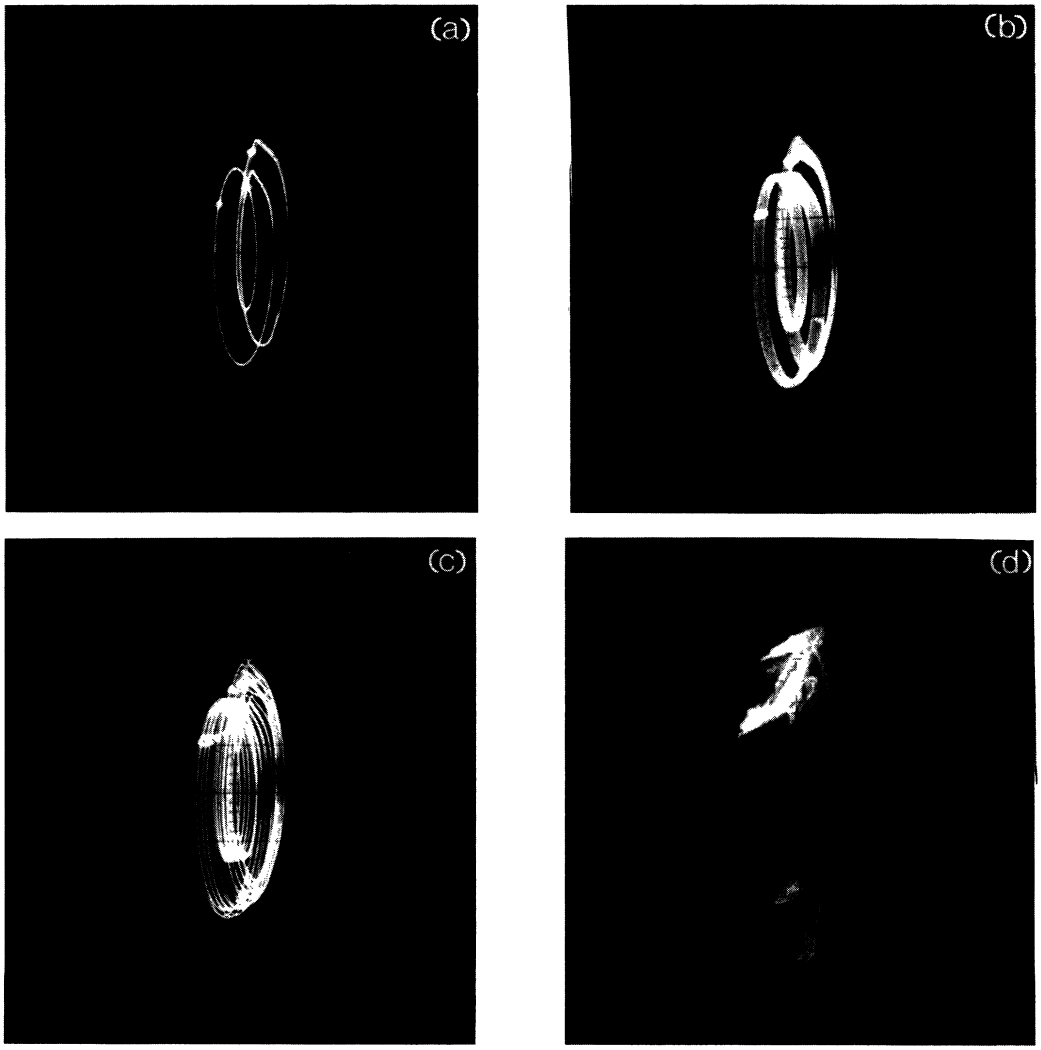

FIG. 2. Sequence of phase plot for the driving amplitude $V_0 \geq 10.50$ V, i.e., after the first transition to chaos. (a) Period-3 state. (b) Quasiperiodic state. (c) Frequency-locked state. (d) Second chaotic state. These plots are pictures taken from the oscilloscope in the X-Y mode, showing the voltage signal $V_1(t)$ across R_1 vs the same signal $V_1(t+\tau)$ with a certain time delay τ. The units of both the X and Y axes are arbitrary.

Lyapunov spectra. The direct calculation of all Lyapunov exponents from an experimental time series of a single observable is a subtle numerical problem. Steady progress in this area has been reported in recent years [9–12]. We used a new algorithm developed by Kruel and Eisworth [12] to study our dynamical system. Guided by the dimensionality of the phase space of the SPICE simulated model we selected $d=3$ and 5 as embedding dimensions for a single diode circuit and a line-coupled system, respectively. Data series we obtained from these systems are well behaved and singular-value decomposition is unnecessary. The obtained spectra of our line-coupled system for typical quasiperiodic and chaotic regimes are listed in Table I. As emphasized by Kruel and Eisworth [12], reliable exponent estimates must be stable in all parameters which enter the program. The two most important parameters are $\epsilon_{\max}$, the maximum distance to locate the neighbors, and t_{evolv}, the evolution time. The exponents listed in Table I have plateaus when $\epsilon_{\max}$ is in the range of [0.01,0.08] and t_{evolve} in the range $[0.5\times10^{-6},9.0\times10^{-6}]$. The maximum variations of the exponents with respect to the above two parameters are entered as the error estimates. We also tried two other algorithms developed by Wolf *et al.* [9] and by Bryant, Brown, and Abrarbanel [11] for the same time series. The positive exponents of the chaotic regimes and the largest negative exponents were all in qualitative agreement.

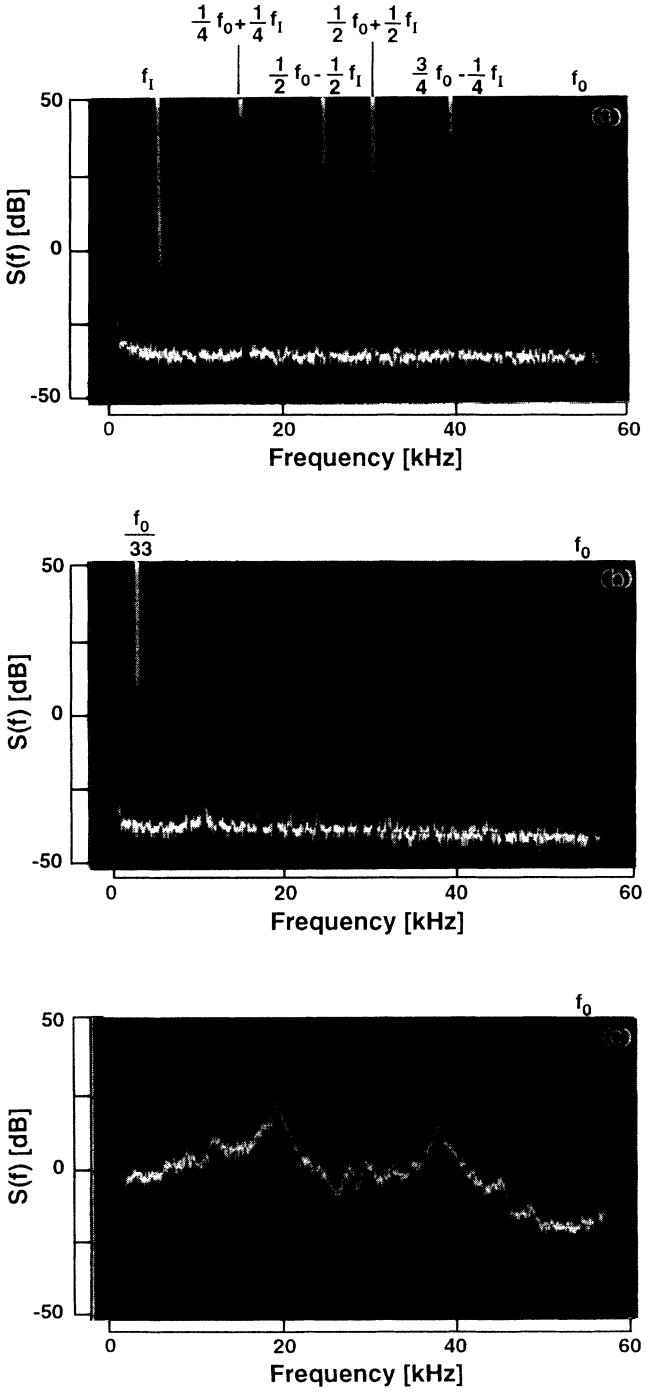

FIG. 3. (a) Power spectrum of the quasiperiodic state shown in Fig. 2(b). Here the two basic frequencies are $f_0\approx50.22$ kHz and $f_I\approx4.43$ kHz. (b) The power spectrum of the frequency-locked state corresponding to the phase plot shown in 2(c). The locking ratio is $\frac{33}{3}$. (c) The power spectrum of the chaotic state corresponding to the phase plot shown in Fig. 2(d).

Less difficult, but by no means trivial, are the calculations of the complete Lyapunov spectra for a simulated model system. In particular, error bars for calculated values may be difficult to estimate and the obtained values may show variations for changing parameters of the algorithm. However, in our simulations we observed high numerical stability of the results with respect to the integration time. Using the diode characteristics model as described in the SPICE program [7] we obtained a set of differential equations with the parameters that match the type of diode and circuit elements we used (see the Appendix for details). After numerical integration of these equations using the Runge-Kutta method for the line-coupled diode system, we found that an identical sequence of transitions, i.e., periodic solution → quasiperiodic solution T^2→frequency-locked state → chaotic state, occurs. Lyapunov spectra calculations based on this model are listed in Table I for comparison with those

TABLE I. Complete Lyapunov spectra of a quasiperiodic regime and a chaotic regime calculated from both experimental time series and SPICE simulated system for our line-coupled diode resonator system.

Experimental time series	Simulated system
Quasiperiodic regime	
−0.0038±0.0002	0.00
−0.0038±0.0006	−0.00175
−0.140±0.015	−0.100
−0.82±0.20	−3.25
−4.0±1.5	−3.27
Chaotic regime	
+0.13±0.02	+0.0876
−0.00170±0.00015	0.00
−0.45±0.08	−0.4
−1.28±0.17	−3.06
−5.96±2.00	−3.42

obtained from the experimental time series. The agreement between the estimated exponents from the experimental data and those calculated from simulated system is very good.

The control circuit we used employed the so-called proportional-feedback technique as discussed by Hunt [3]. The control circuit samples the current peaks, and for all peaks within a preselected adjustable window the difference between peak position and the center of the window is computed, amplified with an adjustable gain, and used as a control signal by a superimposition with the driving sinusoidal signal. The time delay and duration of the control signals are also adjustable parameters of the control circuit.

Now we describe the results obtained by applying this control circuit to a single-diode resonator circuit and to a line-coupled diode resonator system. For a single-diode resonator system we can easily stabilize low-period orbits embedded within the chaotic attractors with appropriate, broad adjustment of the control parameters as mentioned above. The stabilization of high-period orbits is increasingly more difficult (more precise multiparameter tuning required), though we were able to stabilize orbits up to period 17. These results confirm those obtained by Hunt [3] with a somewhat different single-diode circuit and control circuit.

For our line-coupled diode resonator system, we found that the stabilization of high-period orbits is typically easier than in the single-diode system. More importantly, careful stabilization allows one to restore some of *the quasiperiodic orbits* with two incommensurate frequencies. From the point of view of Poincaré maps this obviously is equivalent to the stabilization of an unstable periodic orbit in the Poincaré plane intersecting the attractor. Figures 4(a) and 4(b) indeed show that the controlled quasiperiodic orbit lies within the original attracting set in the Poincaré plane, and the power spectrum in Fig. 5(b) shows that the two incommensurate frequencies are close to those observed in a previously stable quasiperiodic regime. Just near the above control settings, we have obtained a periodic-locked state from the same chaotic attractor. Figure 4(c) shows the phase plot and Poincaré section of this state and its power spectrum in Fig. 5(c) shows that all the peaks are equally spaced. Stabilization of quasiperiodic orbits was possible for a wide variety of line-coupled diode resonator systems with different elements (resistors and inductors) as well as diode types.

We also applied the same control technique to a line-coupled system consisting of four single-diode resonators. This system has periodic, quasiperiodic, and chaotic regimes. The stabilization of periodic and quasiperiodic orbits was also found to be possible, as shown in Fig. 6.

Control signals in the above cases were always small when compared to the system signals (less than 5%). Unfortunately, we cannot provide a simple operational recipe for the stabilization for all of the observed orbits within Hunt's technique. Both high periodic and apparently quasiperiodic orbits are equally difficult to stabilize, and we did not notice any specific difference in the stabilization procedures for orbits of these two types.

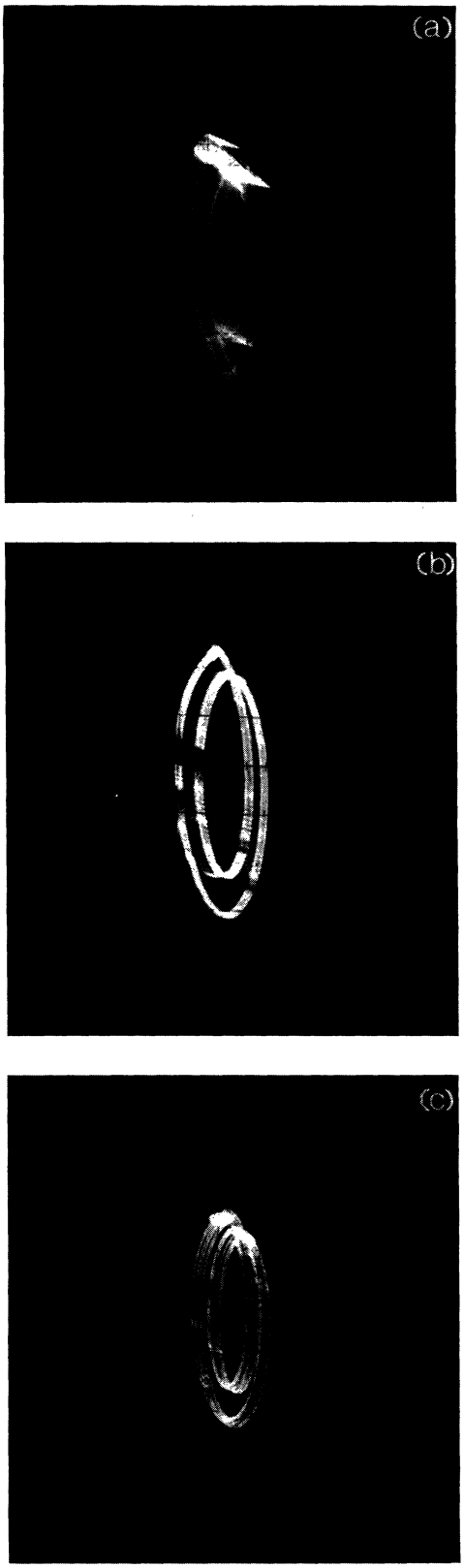

FIG. 4. Phase plot of (a) typical chaotic attractor for 9.90 V $\leq V_0 \leq 10.50$ V, (b) stabilized quasiperiodic state, and (c) stabilized periodic frequency-locked state. As shown in Fig. 2, these plots are pictures taken from the oscilloscope representing $V_1(t)$ vs $V_1(t+\tau)$, and the units of both the X and Y axes are arbitrary.

The orbits classified as quasiperiodic appeared less often than the periodic ones, as may be expected. A word of comment should be added on the observed quasiperiodic orbits. Obviously, a strictly quasiperiodic orbit is an experimental and simulational impossibility (all measured frequencies are commensurate, all simulated orbits are ultimately periodic). Additionally, a high periodic orbit perturbed by a small amount of noise residing on a torus will behave as an almost periodic orbit, which can be well approximated by a quasiperiodic orbit. In this situation, an experimental observation of quasiperiodicity must first localize tori on which these orbits may live, and second provide an example of an orbit which appears dense on this torus. All of our high-period orbits clearly belong to some common tori, similar to those observed in the system before the transition to chaos. Additionally, orbits of period as high as 17 are still classified as such, which indicates the relatively low noise level in the system.

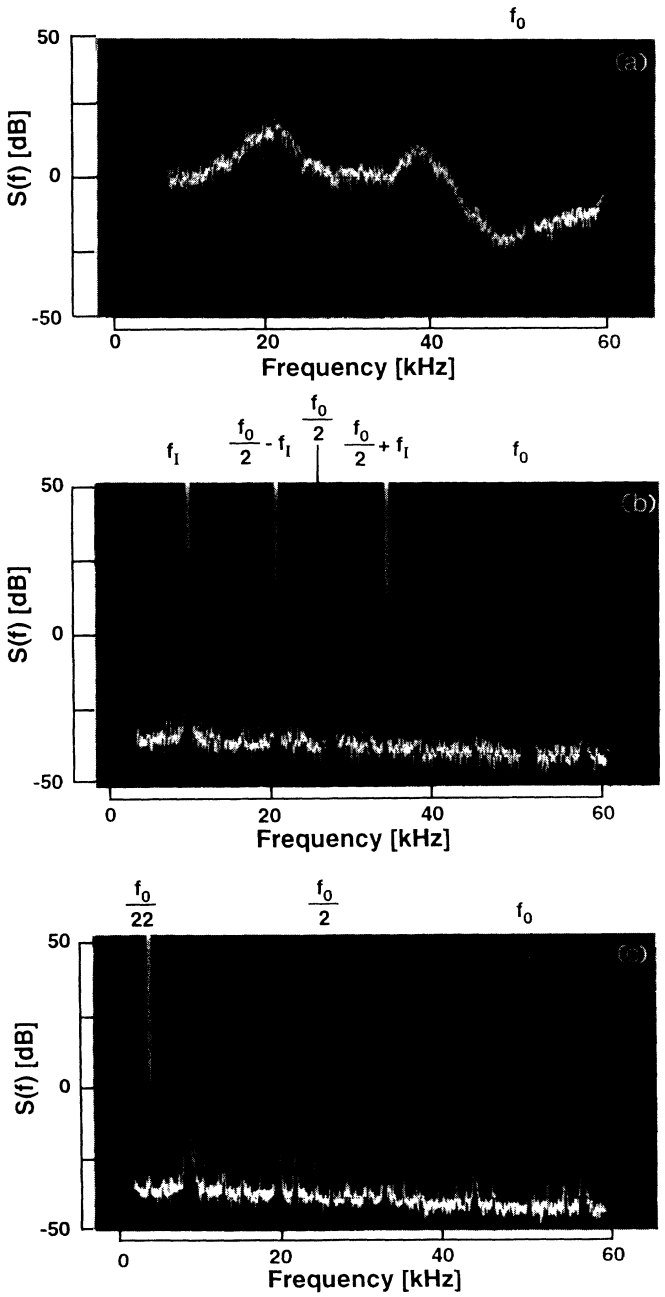

FIG. 5. Respective power spectra for the dynamical regimes of Fig. 4.

In conclusion, systems of coupled, nonlinear diode oscillators have new interesting dynamical features when compared to the single-diode resonator system. Direct transition $T^2 \rightarrow$chaos seems quite common in these systems. The chaotic regimes of these systems can be easily controlled by the proportional-feedback technique. In particular, it is possible to stabilize not only periodic but also quasiperiodic orbits residing on tori. It is well known that a typical chaotic attractor has embedded within it an infinite number of unstable periodic orbits [13]. Based on our stabilization experiments we conjecture that the chaotic attractors for systems we have considered contain both unstable periodic and unstable quasiperiodic orbits.

APPENDIX

The SPICE program models the diode as an ideal diode in parallel with a nonlinear effective capacitor. The nonlinear differential capacitance is modeled as follows:

$$C_D = \frac{dQ_D}{dV_D} = \begin{cases} \tau_D \dfrac{dI_D}{dV_D} + C_d(0)\left|1 - \dfrac{V_D}{\phi_0}\right|^M \\ \text{for } V_D < \mathcal{F}_{\rm FC}\phi_0 \\ \tau_D \dfrac{dI_D}{dV_D} + \dfrac{C_d(0)}{F_2}\left|F_3 + \dfrac{MV_D}{\phi_0}\right| \\ \text{for } V_D \geq \mathcal{F}_{\rm FC}\phi_0 \, , \end{cases}$$

where F_2 and F_3 are

$$F_2 = (1-\mathcal{F}_{\rm FC})^{1+M} \, , \quad F_3 = 1 - \mathcal{F}_{\rm FC}(1+M) \, .$$

The ideal diode is modeled by

$$I_D = \begin{cases} I_s[\exp(qV_D/nKt) - 1] + V_D G_{\min} \\ \text{for } -5\dfrac{nkT}{q} \leq V_D \leq 0 \\ -I_s + V_D G_{\min} \quad \text{for } V_D < -5\dfrac{nkT}{q} \, . \end{cases}$$

Here τ_D, $\mathcal{F}_{\rm FC}(\equiv$FC), $C_d(0)$, M, ϕ_0, n, and $G_{\min}$ are all SPICE constants depending on the diode type.

Ordinary differential equations for our line-coupled diode resonator system in Fig. 1 are listed below. Here the equations were solved using the Runge-Kutta method. I is the current through R_1, I_1 is the current through R_2, V_1, and V_2 are the voltages across the D_1 and D_2 diodes, and V_0 and f are the amplitude and frequency of the driving source. Both resistances are set equal to R_0 and both inductances are equal to L,

$$\frac{dI}{dt} = \frac{V_0 \sin\Omega - V_1 - I(R_0 + R_s)}{L} \, , \tag{A1}$$

$$\frac{dI_1}{dt} = \frac{V_0 \sin\Omega - 2V_1 + V_2 - I_1(R_0 + R_s)}{L} \, . \tag{A2}$$

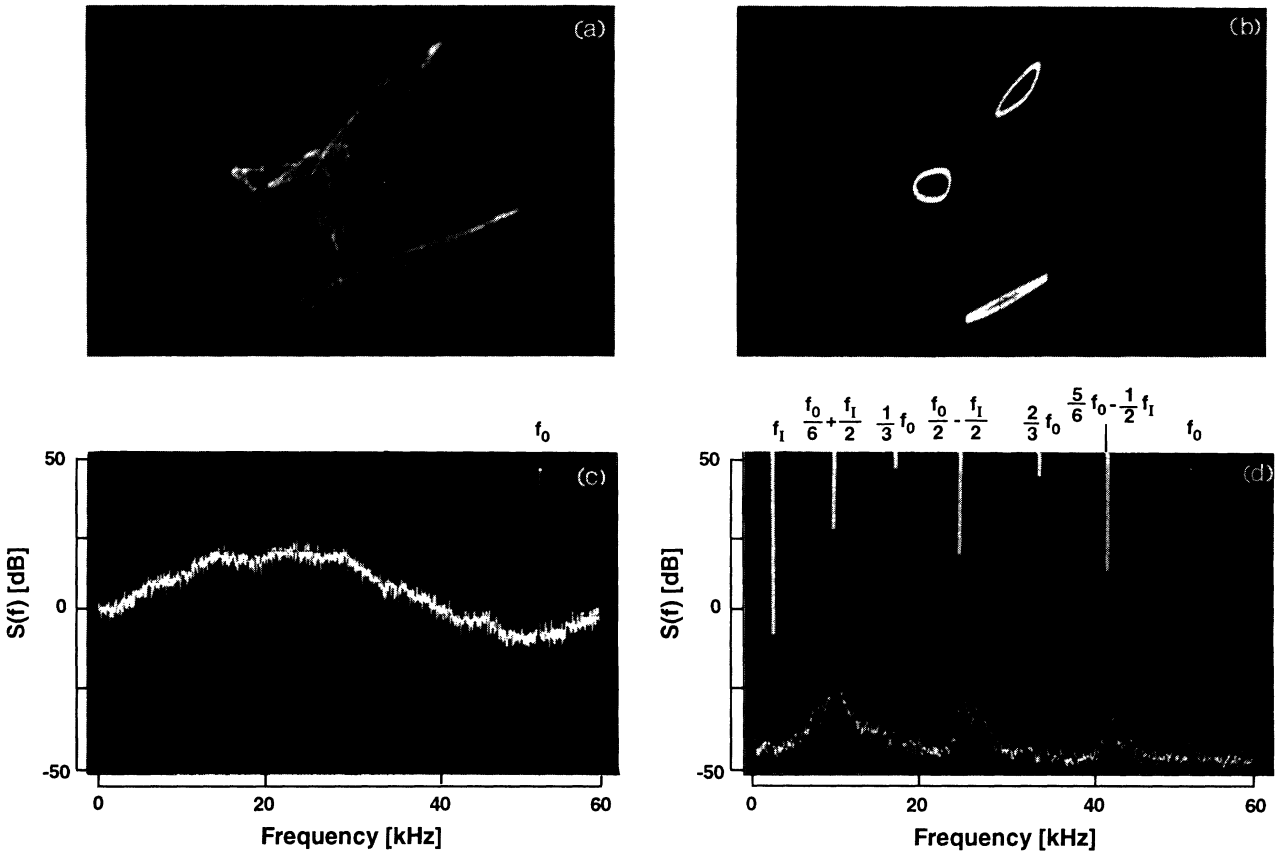

FIG. 6. (a) Phase plot of a chaotic attractor from four line-coupled diode resonators. (b) Stabilized quasiperiodic state from the above chaotic attractor. (c) and (d) are their power spectra.

$$\frac{dV_1}{dt}=\begin{cases}\dfrac{I_1-I_{d1}}{\tau_d\dfrac{dI_{d1}}{dV_1}+C_d(0)\left[1-\dfrac{V_1}{\phi_0}\right]^{-M}} & \text{when } V_1<\mathcal{F}_{\mathrm{FC}}\phi_0 \\ \dfrac{I_1-I_{d1}}{\tau_d\dfrac{dI_{d1}}{dV_1}+\dfrac{C_d(0)\left[F_3+\dfrac{MV_1}{\phi_0}\right]}{F_2}} & \text{when } V_1\geq\mathcal{F}_{\mathrm{FC}}\phi_0\ ,\end{cases} \tag{A3}$$

$$\frac{dV_2}{dt}=\begin{cases}\dfrac{I-I_1-I_{d2}}{\tau_d\dfrac{dI_{d2}}{dV_2}+C_d(0)\left[1-\dfrac{V_2}{\phi_0}\right]^{-M}} & \text{when } V_2<\mathcal{F}_{\mathrm{FC}}\phi_0 \\ \dfrac{I-I_1-I_{d2}}{\tau_d\dfrac{dI_{d2}}{dV_2}+\dfrac{C_d(0)\left[F_3+\dfrac{MV_2}{\phi_0}\right]}{F_2}} & \text{when } V_2\geq\mathcal{F}_{\mathrm{FC}}\phi_0\ ,\end{cases} \tag{A4}$$

$$\frac{d\Omega}{dt}=2\pi f\ , \tag{A5}$$

where

$$I_{d1}=I_s[\exp(V_1/NkT)-1]+V_1G_{\min}\ ,\quad I_{d2}+I_s[\exp(V_2/NkT)-1]+V_2G_{\min}\ .$$

[1] E Ott, C. Grebogi, and J. A. Yorke, Phys. Rev. Lett. **64**, 1196 (1990).

[2] W. L. Ditto, S. N. Rauseo, and M. L. Spano, Phys. Rev. Lett. **65**, 3211 (1990); J. Singer, Y-Z. Wang, and H. H. Bau, *ibid.* **66**, 1123 (1991); A. Azevedo and S. M. Rezende, *ibid.* **66**, 1342 (1991); Y. Braiman and I. Goldhirst, *ibid.* **66**, 2545 (1991); R. Lima and M. Pettini, Phys. Rev. A **41**, 726 (1990).

[3] E. R. Hunt, Phys. Rev. Lett. **67**, 1953 (1991).

[4] J.Testa, J. Perez, and C. Jefferies, Phys. Rev. Lett. **48**, 714 (1982).

[5] R. Buskirk and C. Jeffries, Phys. Rev. A **31**, 3332 (1985).

[6] J. Curry and J. A. Yorke, *The Structure of Attractors in Dynamical Systems*, Lecture Notes in Mathematics, Vol. 668 (Springer-Verlag, Berlin, 1977), p. 48. See also P. Bergé, Y. Pomeau, and C. Vidal, *Order within Chaos, Towards a Deterministic Approach to Turbulence* (Hermann, Paris, 1984), p. 168 (translated from the French by L. Tuckerman).

[7] SPICE, Department of Electrical Engineering and Computer Sciences, University of California at Berkeley. See also Paolo Antognetti and Giuseppe Massobrio, *Semiconductor Device Modeling with SPICE* (McGraw-Hill, New York, 1988).

[8] See, e.g., D. Ruelle, *Chaotic Evolution and Strange Attractors* (Cambridge University Press, Cambridge, 1989).

[9] A. Wolf, J. B. Swift, H. L. Swinney, and J. A. Vastano, Physica **16D**, 285 (1985).

[10] M. Sano and Y. Sawada, Phys. Rev. Lett. **55**, 1082 (1985).

[11] P. Bryant, R. Brown, and H. D. I. Abrarbanel, Phys. Rev. Lett. **65**, 1523 (1990).

[12] Th.-M. Kruel, M. Eisworth, and F. W. Schneider, Physica **63D**, 117 (1993).

[13] C. Grebogi, E. Ott, and J. A. Yorke, Phys. Rev. A **37**, 1711 (1988).

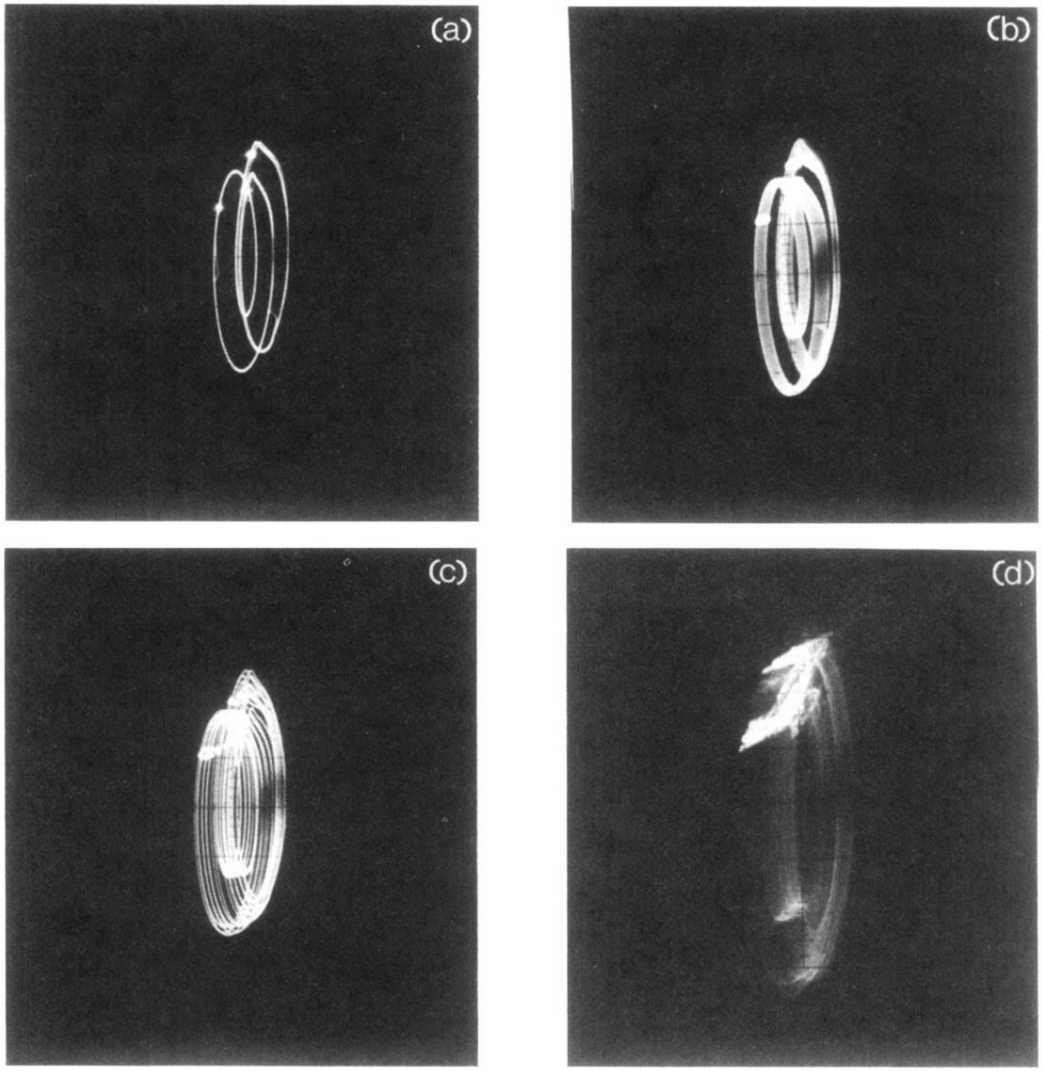

FIG. 2. Sequence of phase plot for the driving amplitude $V_0 \geq 10.50$ V, i.e., after the first transition to chaos. (a) Period-3 state. (b) Quasiperiodic state. (c) Frequency-locked state. (d) Second chaotic state. These plots are pictures taken from the oscilloscope in the X-Y mode, showing the voltage signal $V_1(t)$ across R_1 vs the same signal $V_1(t+\tau)$ with a certain time delay τ. The units of both the X and Y axes are arbitrary.

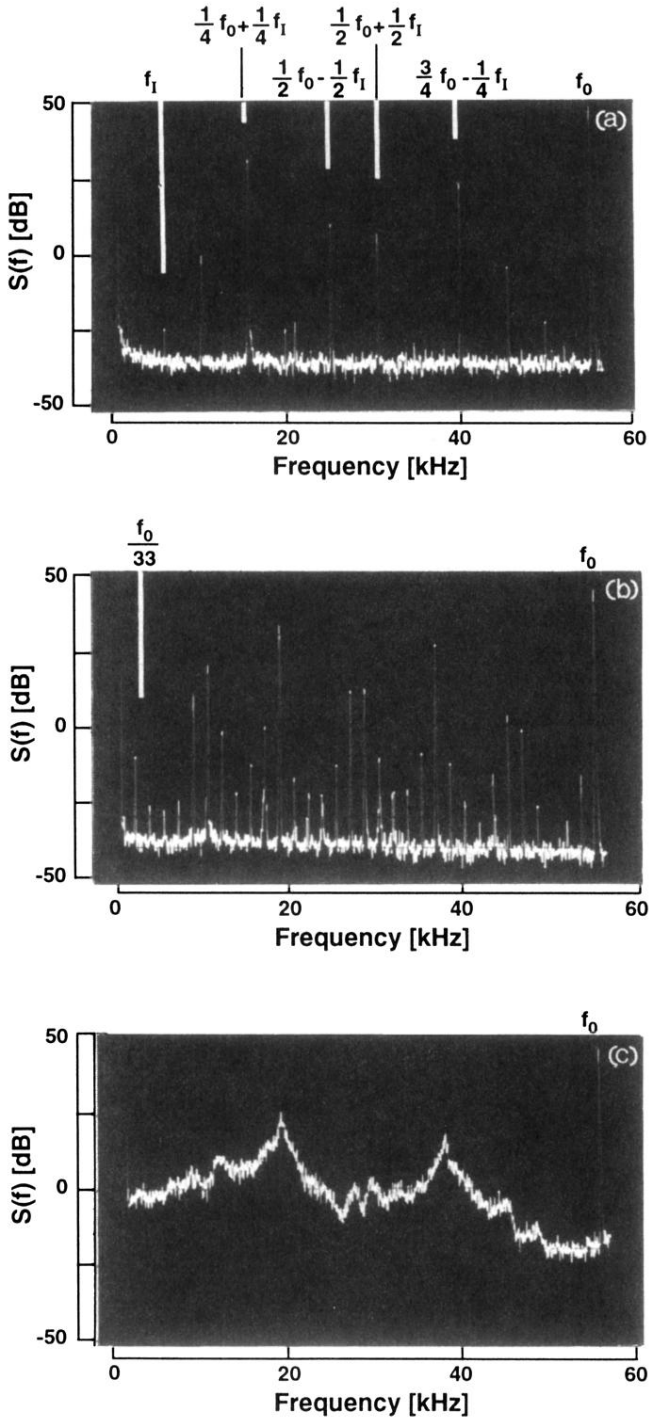

FIG. 3. (a) Power spectrum of the quasiperiodic state shown in Fig. 2(b). Here the two basic frequencies are $f_0 \approx 50.22$ kHz and $f_i \approx 4.43$ kHz. (b) The power spectrum of the frequency-locked state corresponding to the phase plot shown in 2(c). The locking ratio is $\frac{33}{3}$. (c) The power spectrum of the chaotic state corresponding to the phase plot shown in Fig. 2(d).

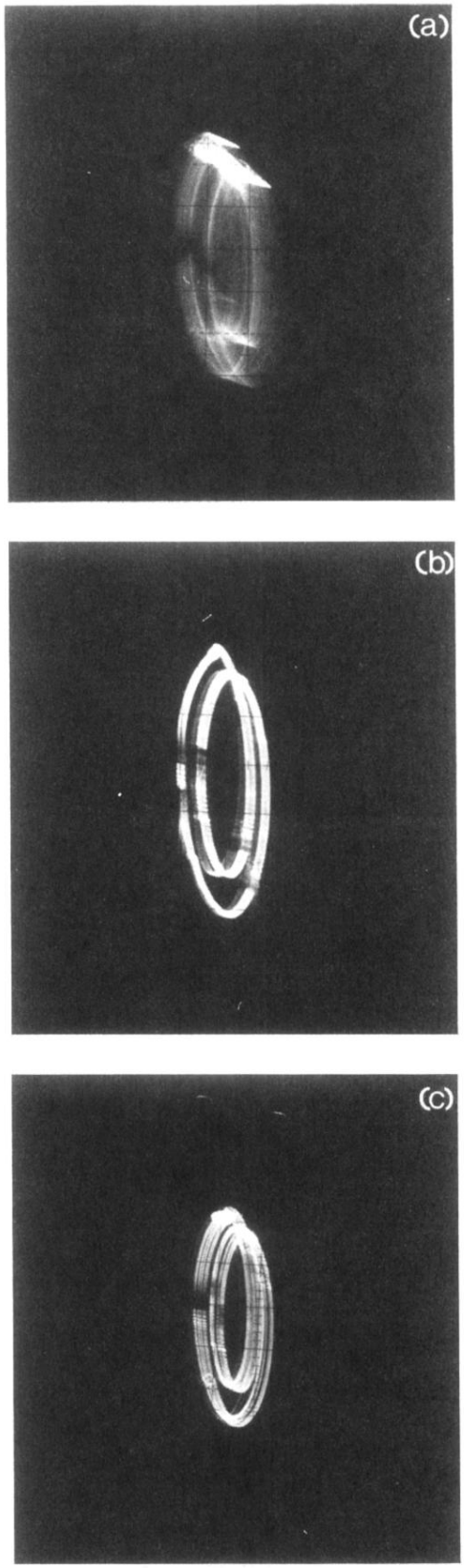

FIG. 4. Phase plot of (a) typical chaotic attractor for 9.90 V $\leq V_0 \leq 10.50$ V, (b) stabilized quasiperiodic state, and (c) stabilized periodic frequency-locked state. As shown in Fig. 2, these plots are pictures taken from the oscilloscope representing $V_1(t)$ vs $V_1(t+\tau)$, and the units of both the X and Y axes are arbitrary.

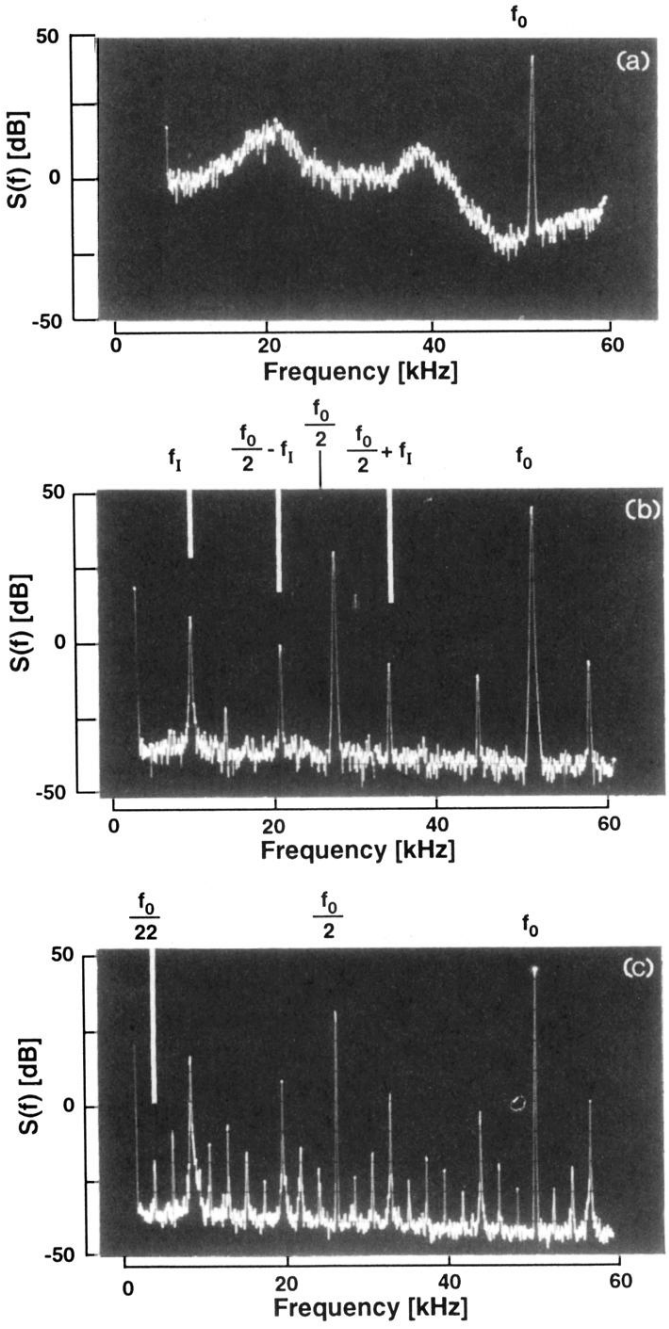

FIG. 5. Respective power spectra for the dynamical regimes of Fig. 4.

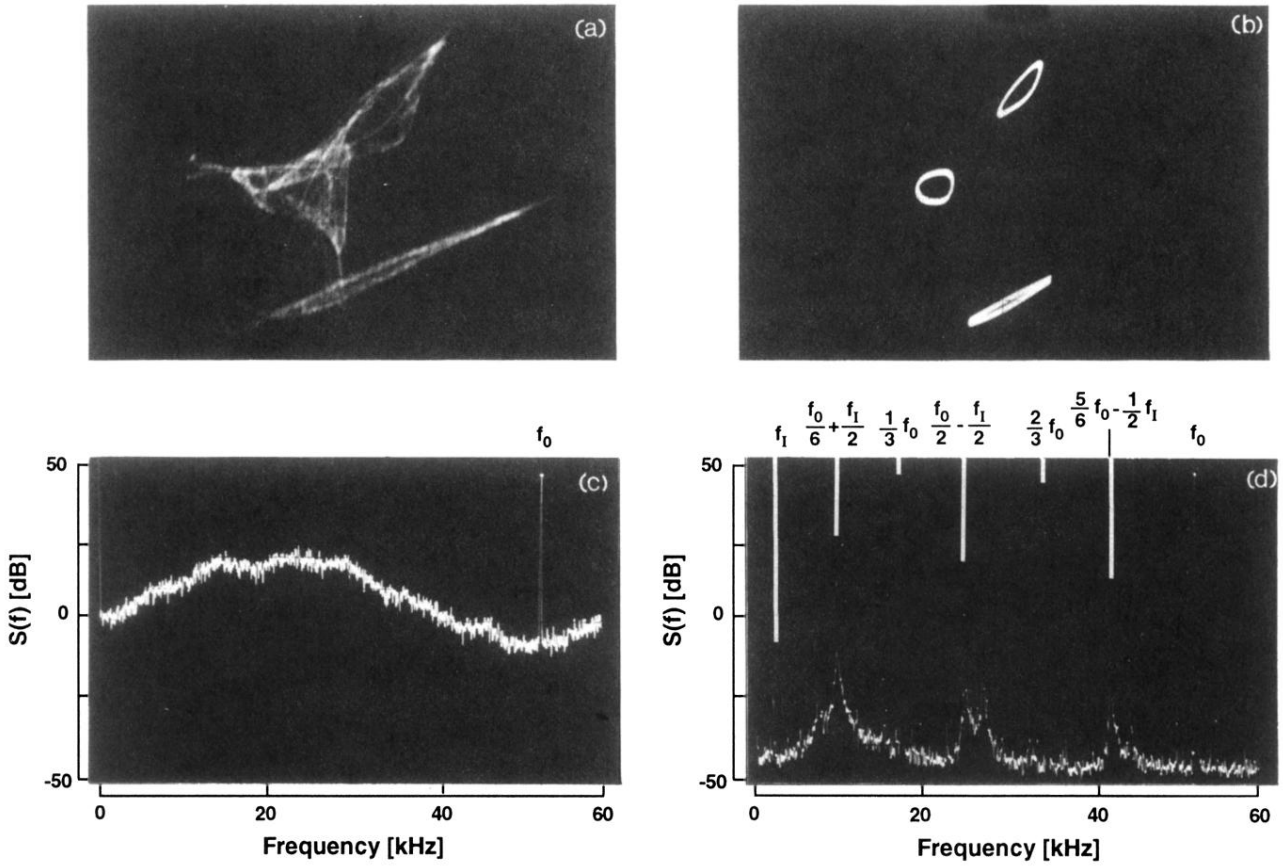

FIG. 6. (a) Phase plot of a chaotic attractor from four line-coupled diode resonators. (b) Stabilized quasiperiodic state from the above chaotic attractor. (c) and (d) are their power spectra.